3D-Engineered Muscle Tissue as a Wireless Sensor: AntennAlive

Cagla Karabulut, Ahmet Bilir, Macit Emre Lacin, and Sema Dumanli

S ynthetic biology has the potential to drastically change sensor technologies. Living cells can now be genetically programmed to be responsive to specific molecules. If those living cells are supported to live inside a host body, in vivo sensing at a molecular level can be achieved. However, the communication link between the genetically modified cells and the outside of the host body is an open area of research. Here, we propose a generic wireless communication platform that we call *AntennAlive* to bridge this gap. The link described can be considered as a gateway between the molecular links that are used by living cells and electromagnetic links. It is a groundbreaking proposition that will initiate a new area of research where antenna design meets synthetic biology. As an example, a biohybrid implant consisting of engineered skeletal muscle and a reconfigurable implant antenna is described. The implant antenna is used as a passive reflector that is reconfigured by the contraction of the skeletal muscle initiated with a trigger molecule that we are

interested in sensing. This reconfiguration is tracked by an on-body reader that completes the wireless link. Note that here sensing is realized with skeletal muscle for the first time in the literature.

INTRODUCTION

The landscape of the medical diagnostics field is being rapidly transformed by implant wireless biomedical devices. These devices are used for monitoring, diagnostics, or therapy purposes. Monitoring devices aim for various applications, such as capsule endoscopy [1], [2], brain–computer interfaces [3], and glu-

cose [4], [5], pH [6], [7], and internal pressure monitoring [8]. Most of these biomedical sensors have a limited lifetime because of their power requirements. Most of these in vivo devices monitor physical parameters and are not specific to certain molecules that might be needed to monitor specific diseases. In the literature, real-time in vivo sensors have been proposed before, such as electromagnetic glucose-sensing systems. However, they aim to sense the secondary effects of the glucose, such as an increase in the tissue permittivity [9], [10], [11], [12], [13].

Molecular-level sensing may open doors for high-sensitivity diagnostics. Electrochemical biosensors with such molecular sensing capabilities are well studied in the literature [14], [15]. Nanostructure-based biosensors [16], [17] are also recently emerging. However, unless molecular sensing is conducted in vivo, the sensors cannot offer wireless real-time detection in the patient's body, whereas the system proposed in this work can directly detect the target molecule itself. Although rare, there are examples of molecular-level sensing in vivo utilizing bacterial cells [18], [19]. This is achieved with the possibilities created by synthetic biology [20], [21], [22], [23], which provides us with the tools to reprogram living cells. Living cells, bacterial or mammalian, can be reprogrammed to operate as sensors [18], [24], [32]. Cells detect and respond to stimuli. Synthetic biology allows us to manipulate the genetic circuitry of cells, enabling the creation of transgenic sensors that are specific for certain molecular stimuli [24]. To practically take advantage of living cells for sensing at a molecular level, the response of the cell upon detection should be translated to a readout signal that can be recognized by humans. One of the most commonly used responses is an optical one, so that the detection is visible to the human eye [29]. Using these sensors as implant sensors would be ideal considering that a host body would support the best lifetime for such a cell-based sensor. However, the propagation depth of visible light in the human body is extremely low, proving the commonly used optical response invalid. Here we propose a solution that connects the response of the cell to the outside world through microwaves so that such a cell-based sensor can be used as an implant and be wirelessly connected. The main obstacle is that microwaves are not suitable to sense the response of the cells directly. The reason is that the changes that occur at the cellular scale are typically in the angstrom ranges, which would require high-frequency electromagnetic waves, such as X-rays. Hence, a conversion is needed where the response of the cells is translated into a change

that can be detected with microwaves. In the proposed system, this conversion is achieved by reconfiguring a passive implant antenna. Reconfigurable implant antennas have been proposed in the literature previously, where vias and pin diodes were utilized to reconfigure the implant antenna's radiation pattern [25], [26], polarization [27], and resonant frequency [28]. Such devices require a power unit to realize the reconfiguration task. The proposed work eliminates the need for a physical power unit by pushing the reconfiguration and sensing tasks to living cells.

Here, we propose a novel sensing mechanism that can achieve sensing at a molecular level in vivo using mammalian cells for the first time [30]. While skeletal muscle tissue has previously been used to actuate biohybrid devices, such as micromotors [34], [35], [36], walking and swimming robots [37], and pumps [39], or for disease modeling and pharmacological testing on organ-on-a-chip platforms [40], our work will be the first in employing skeletal muscle tissue for biosensing. This has various advantages over conventional implant sensors, such as self-repair and replacing electrical energy sources with adenosine triphosphate (ATP) [41], [24].

Skeletal muscle tissue with its contractile response offers a novel biosensor type. Note that this study is not only novel in the utilization of skeletal muscle as a sensor, but it is also the first time the

skeletal muscle is used as an implant. Moreover, molecular in vivo sensing by mammalian cell-based biosensors has never been achieved. A comparison of this study with the state of the art is presented with a lotus graph in Figure 1. The development of such implant biosensors with molecular sensing capabilities will have a profound impact on the medical field. It has the potential to be the ultimate interface between the way cells communicate and electromagnetic communications.

The rest of the article is organized as follows: in the next section, the details of the sensing mechanism and the muscle tissue development are given. In the section "Numerical Models," the sensing is mechanically and electromagnetically modeled. In the section "Measurements," the measurement setup is detailed, and in the section "Results and Discussion," the simulation and measurement results are discussed. Finally, the section "Conclusions" concludes the work.

BIOHYBRID IMPLANT

In the proposed mechanism, the sensing is mainly realized by a biohybrid device. The device consists of an implant antenna that is reconfigured by 3D-engineered skeletal muscle tissue and a 3D-printed flexible scaffold that supports both the implant antenna and the growth of the skeletal muscle tissue.
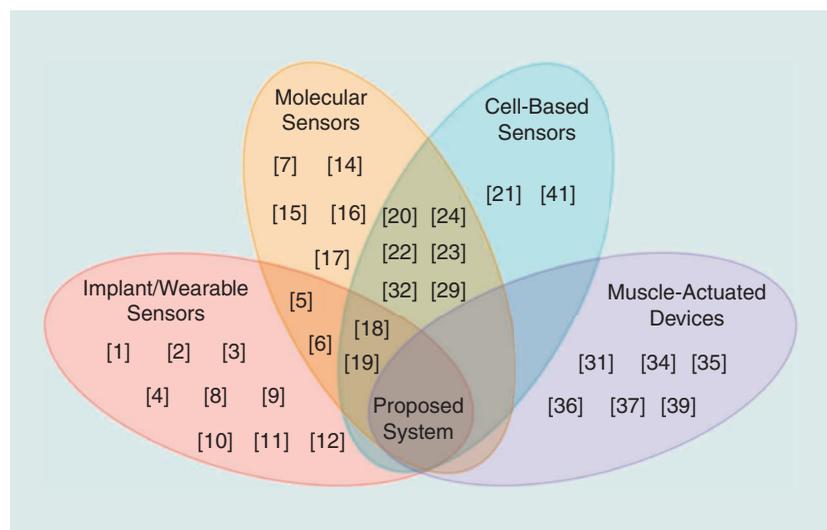

FIGURE 1. An overview of the state of the art.

THE SENSING MECHANISM

The skeletal tissue lives inside the flexible scaffold and reports the presence of the trigger molecule via its contractile output. The flexible scaffold consists of a microwell with two thin pillars anchored to its bottom, one of which has a conductive bridge extending toward the implant antenna. The bridge operates as an electrical switch. In the presence of a molecule of interest, the switch is toggled and the resonance of the implant antenna gets switched from one state to another, as seen in Figure 2. The implant antenna is formed by coating the top surface of the 3D-printed scaffold with conductive ink.

An overview of the architecture and the system components is given in Figure 2. When the engineered skeletal tissue comes in contact with the trigger molecule, the muscle will sense the molecule and contract. Note that for the muscle to contract upon reception of the target molecule, it should be genetically modified. To induce a muscle contraction in the presence of a specific molecule, this molecule should control the ion channels. For example, if we considered glucose as a trigger molecule, the following procedure could have been realized: glucose transporter 2 and the ATP-sensitive potassium (KATP) channel can be overexpressed into the muscle cells to induce muscle contraction in the presence of glucose. The KATP channel will be in an open state in glucose deficiency, where the membrane potential can be preserved. In the presence of glucose, however, the presence of the synthesized ATP will increase. As a result, the KATP channel will be switched to a closed state, and the membrane will be depolarized, leading to the contraction of the muscle. Note that this is just an example and a full discussion is beyond the scope of this work. Here we aim to demonstrate the feasibility of this novel sensing platform and its wireless communication. This technique will be limited to the advancements in synthetic biology [44]. The contraction with the trigger molecule will toggle an electrical switch and change the resonant frequency of the biohybrid implant antenna. The change in the resonant frequency is tracked by a wideband dual-port on-body antenna. In this way, the arrival of the trigger molecule is wirelessly tracked in real time.

3D-ENGINEERED SKELETAL MUSCLE TISSUE

The engineered skeletal muscle tissue is considered as the interface of the molecular links, while the implant antenna is the interface of the electromagnetic links to the outside world. Therefore, the system works as a multiscale communications platform that bridges an existing gap between the molecular links and the on-body devices that can relay the information to the outside world.

The C2C12 immortalized mouse myoblast cell line is used to generate 3D-engineered muscle tissues by following the protocol explained in [43]. This protocol involves maintaining the cells in a growth medium (GM), harvesting them once they reach a certain confluency, and then resuspending them in a mixture of collagen and Matrigel. This mixture is then loaded into a 3D-printed flexible scaffold and incubated for 1–2 h. The gel inside the scaffold is then overlaid with the GM and left for two days. On the second day, the GM is replaced with a low-serum differentiation medium (DM), and the cells are left to differentiate for an additional 12–14 days. The goal of this protocol is to generate mature skeletal muscle tissues that can be used in various applications. Once the skeletal muscle tissues are matured at the end of the 3D differentiation period, the tissues are tested to validate their functionality, as will be detailed in the section "Skeletal Muscle Tissue Functionality Tests." Acetylcholine (ACh) is a known natural muscle stimulant, and healthy muscle fibers respond to it by generating a contraction movement [45]. We chose ACh as our trigger
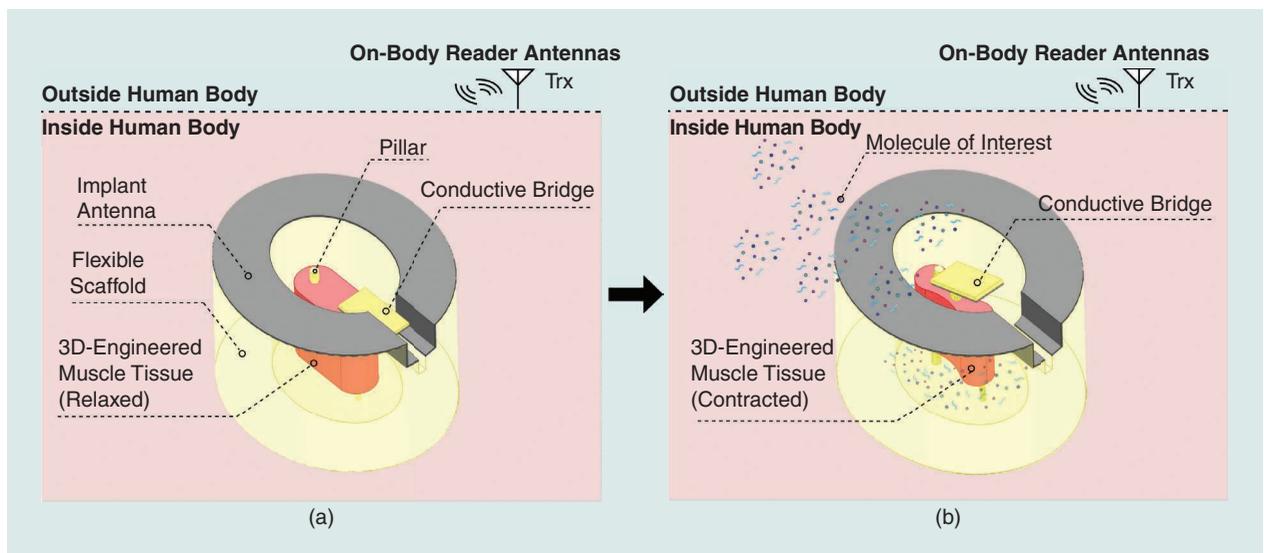
FIGURE 2. The architecture of the sensing system and the biohybrid implant components. (a) Relaxed. (b) Contracted. Trx: transceiver.

molecule. It is envisaged that the trigger molecule can be replaced by any molecule of interest, such as biomarkers of certain health conditions in the future.

Note that the C2C12 cell line is immortalized, which means that, under ideal maintaining conditions, it can multiply indefinitely without undergoing senescence. Therefore, using the immortalized line of C2C12 eliminates the need to sacrifice animals, and it is less costly to grow and maintain the C2C12 tissues.

FLEXIBLE SCAFFOLD AND IMPLANT ANTENNA DESIGN

While facilitating the implant antenna and the switching mechanism, the flexible scaffold also provides structural support to the skeletal muscle tissue. During the early stages of differentiation, C2C12 myoblasts start forming fiber-like structures in two dimensions. Without external structural support, the tissue fibers cannot align themselves vertically and remain planar. To provide the required structural support to the 2D tissue fibers, we engineer tendon-like interfaces that mimic the tendon and bone structures of the native musculoskeletal system, which is our 3D-printed flexible scaffold implant.

The scaffold dimensions and material are optimized to result in maximum deflection against the minimal external forces generated by the muscle tissue. The proposed flexible scaffold and the implant antenna dimensions are as shown in Figure 3(a) and (b). It can be observed that, for such a structure, high resolution and accuracy are required. The stereolithography (SLA) 3D printing method uses a light source, such as a laser or a projector, to cure liquid resin into hardened plastic objects with a desired stiffness. Since this printing method uses light to shape its printing materials, SLA-printed parts have higher resolution and accuracy, sharper details, and smoother finishes than those obtained with most of the other 3D printing methods. Therefore, SLA 3D printing is utilized, and it is highly flexible and biocompatible. Formlabs IBT resin is chosen as the printing material.

SKELETAL MUSCLE TISSUE FUNCTIONALITY TESTS

To observe the contraction of the muscle tissue, the biohybrid implant is placed in a six-well plate under an inverted microscope. During the test phase, the C2C12 cells are sequentially stimulated by adding 100 μM ACh dissolved in phosphate-buffered saline (PBS). In between muscle stimulants pulses, the biohybrid implant well is washed with PBS. The tissue contraction is tracked with a digital microscope camera, and ImageJ software [38] is used to determine the contraction in arbitrary units by quantifying and comparing the visible area of the tissue when it is relaxed and contracted, as seen in Figure 4(a). Figure 4(b) shows the matured skeletal tissue subjected to the ACh test.

NUMERICAL MODELS

MECHANICAL MODEL

The biohybrid device design is mechanically simulated to analyze the scaffold deflections against contractile forces that can be generated by the skeletal muscle tissue. The mechanical simulations
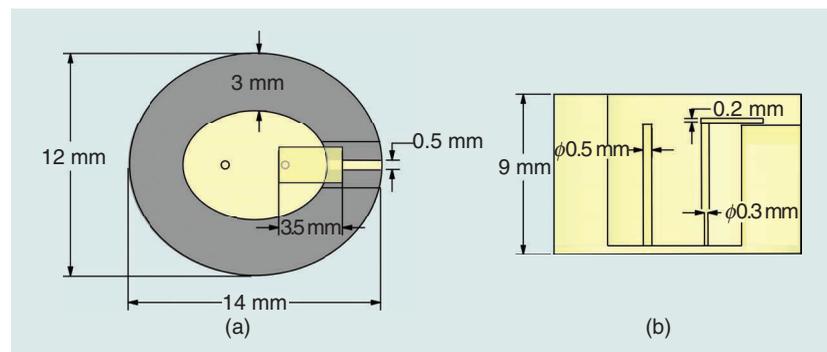

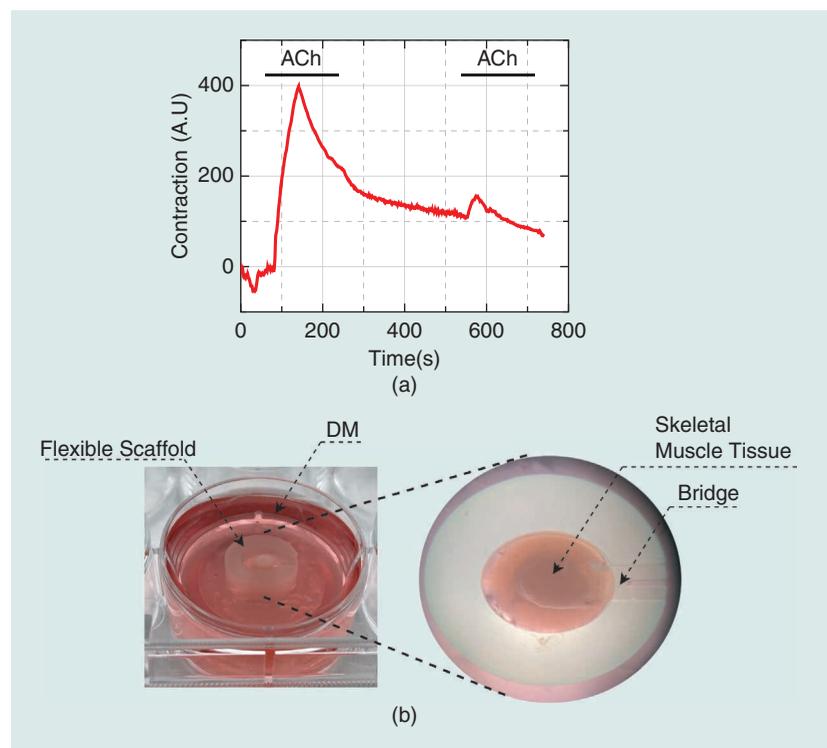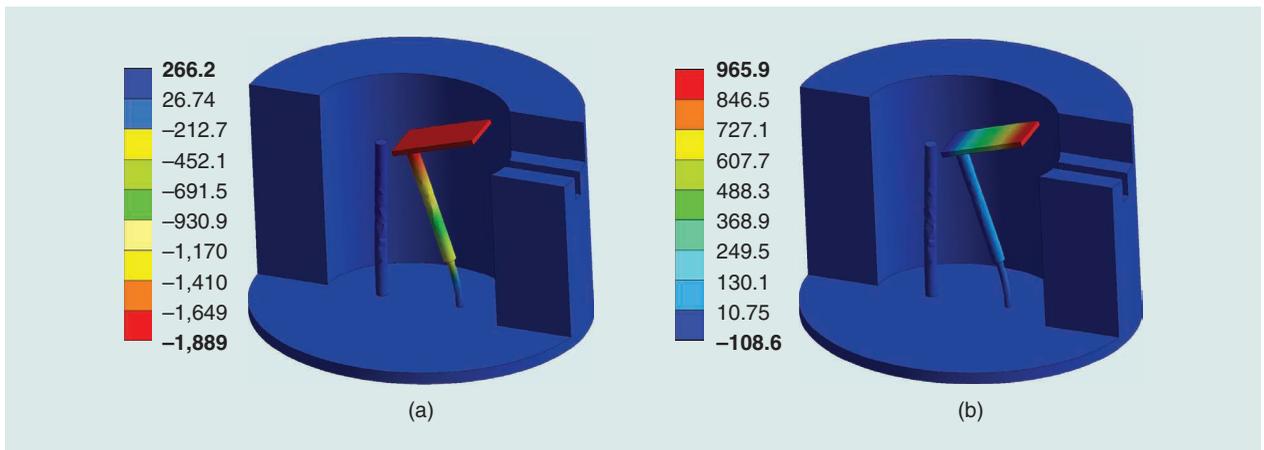**FIGURE 3.** Biohybrid implant dimensions. (a) Top view. (b) Side view.

FIGURE 4. Functional 3D-engineered skeletal muscle tissue. (a) Motion trace showing muscle contraction and relaxation on two ACh pulses. (b) Matured skeletal muscle tissue subjected to the ACh test.
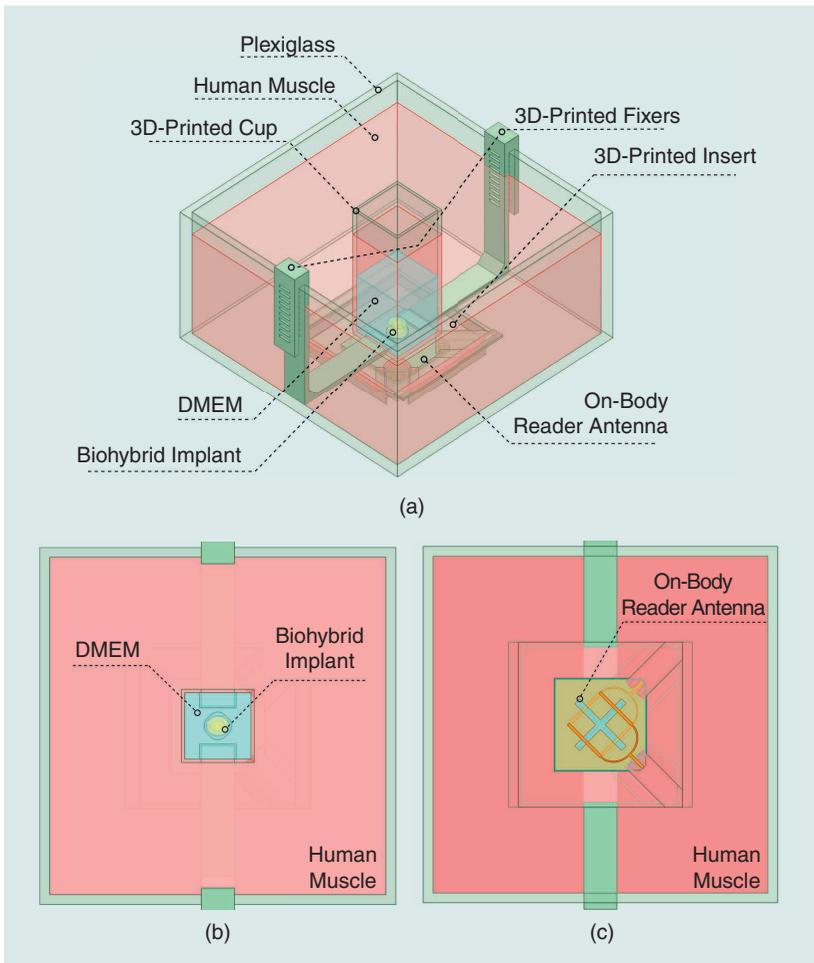
FIGURE 5. Mechanical deflection analysis of the flexible scaffold. (a) Deflection in *x* direction. (b) Deflection in *z* direction (in *μ*m).

are characterized using the mechanical properties of IBT. This resin is a polymer-based elastic material with an ultimate tensile strength and elasticity modulus that are greater than 5 MPa and 16 MPa, respectively [33]. In the literature, the 3D-engineered skeletal muscle tissues were shown to generate contraction forces from 10 *μ*N to 2.5 mN [13]. Therefore, 300 *μ*N is applied to both pillars in the *x* and –*x* directions. The maximum deflection of the conducting bridge is observed to be 1,889 *μ*m and 965.9 *μ*m in the –*x* and *z* directions, respectively, as seen in Figure 5(a) and (b). Note that in these figures, a portion of the flexible scaffold outer walls is shown clipped for visibility purposes. To demonstrate the gradual change in tissue contraction and the conductive bridge deflection, the mechanical analysis is also conducted for intermediate force values, namely 50 *μ*N and 100 *μ*N. Against 50 *μ*N of applied force, the maximum deflection of the bridge is observed to be 245 *μ*m and 121 *μ*m in the –*x* and *z* directions, respectively. Against 100 *μ*N of applied force, the maximum deflection of the bridge is observed to be 533 *μ*m and 271 *μ*m in the –*x* and *z* directions, respectively. The output of the mechanical simulations is inputted to the Ansys high-frequency structure simulator for electromagnetic simulations, which will be discussed in the next section.

ELECTROMAGNETIC MODEL

The biohybrid implant is electromagnetically modeled, as seen in Figure 6. Its behavior inside a numerical phantom as the muscle contracts is simulated. The numerical phantom consists of two different layers: muscle tissue and interstitial fluid. The biohybrid implant is located inside the interstitial fluid at a depth of 1 cm.

To track the switching action generated by the engineered muscle, a dual-port, wideband on-body antenna is designed, as seen in Figure 7. The ports of the antenna excite two orthogonal modes of a cross-slot antenna. The coupling between the ports is lower than

FIGURE 6. Electromagnetic model of the measurement setup. (a) Isometric view. (b) Top view. (c) Bottom view. DMEM: Dulbecco's Modified Eagle's Medium.

–30 dB for the frequency band of the operation, from 900 MHz to 2.5 GHz. The band of operation is chosen to be wide so that the reading mechanism is immune to the detuning effects of the human body on the implant antenna. The overall size of the antenna is 55 × 55 × 3.9 mm [42]. The antenna performs effectively within the desired frequency range for tissues with a relative permittivity greater than 30. The reason is that the radiator is situated between the microstrip feeds and a low-loss dielectric substrate, making the antenna resistant to detuning. The results for the electromagnetic simulation are presented in Figure 8.

MEASUREMENTS

As shown in Figure 9, the electromagnetic measurement setup consists of a plexiglass container of size 20 cm × 20 cm × 12 cm, a 3D-printed square prism cup of size 4 cm × 4 cm × 10 cm, and 3D-printed height-controlled fixers. The 3D-printed cup is fixed to the center of the plexiglass container at a depth of 90 mm with the 3D-printed height-controlled fixers, and it is filled with Dulbecco's Modified Eagle's Medium (DMEM). The volume between the plexiglass container and the 3D-printed cup is filled with human muscle phantom. The biohybrid implant is placed at the bottom of the 3D-printed cup. The bottom of the 3D-printed cup is 1 mm thick, and it is located at a 10-mm distance from

the on-body reader antenna. The on body-reader antenna is placed at the bottom of the plexiglass container with the 3D-printed insert.

The measurements for the proposed sensing system were carried out inside the fabricated tissue-mimicking phantoms that were used in the
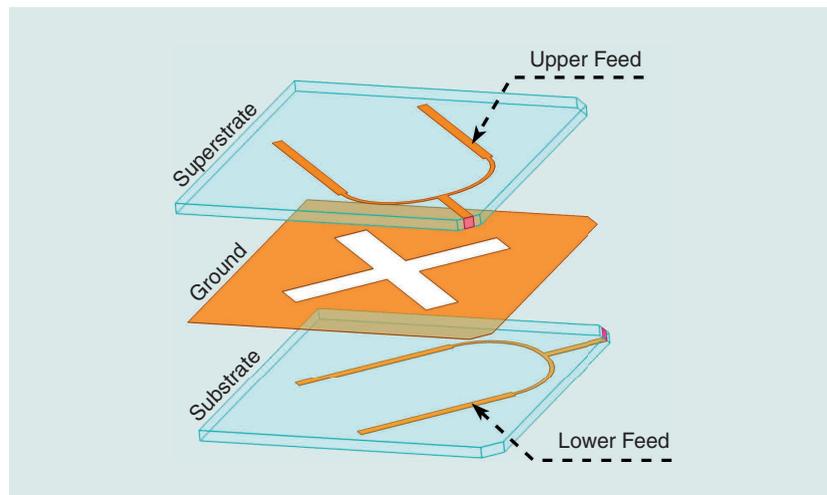
FIGURE 7. Exploded view of the on-body reader antenna.
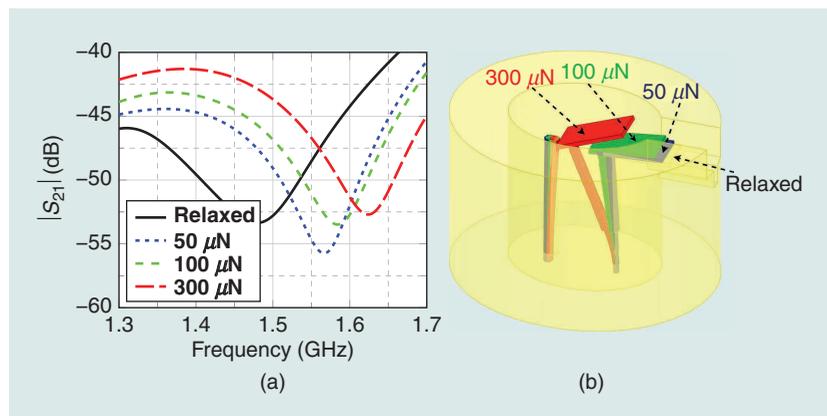

FIGURE 8. Electromagnetic simulation results. (a) Change in $|S_{21}|$ against the gradual contraction of the tissue. (b) Gradual contraction of the tissue.

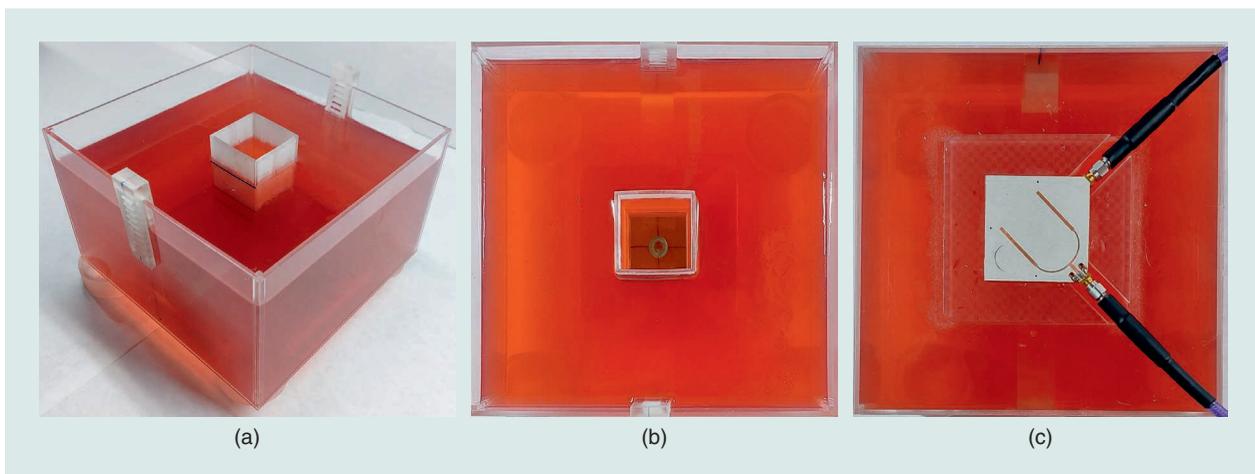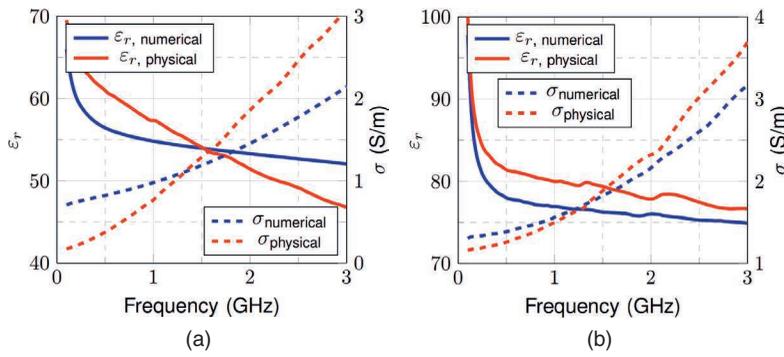
FIGURE 9. Electromagnetic measurement setup: the physical phantoms, on-body reader antenna, and implant antennas mimicking reconfiguration under skeletal muscle contraction. (a) Isometric view. (b) Top view. (c) Bottom view.

FIGURE 10. ε_r and σ of the numerical and physical phantoms versus frequency. (a) Human muscle. (b) DMEM.

electromagnetic analysis. The physical phantom for Ansys human muscle was

TABLE 1. THE INGREDIENTS USED FOR THE PHYSICAL PHANTOMS PER UNIT VOLUME.

Ingredient	Ansys Human Muscle	DMEM
Tap water	100 mL	100 mL
Salt	0.2 g	0.8 g
Granulated sugar	60 g	—
Gelatin	9 g	—
Sodium azide	0.3 g	—
Food coloring gel	40 drops	—

fabricated using water, granulated sugar, gelatin, sodium azide, and food coloring gel. The maximum deviation of the permittivity and the conductivity of the human muscle phantom is 4.62% and 27.9%, respectively, within the band of interest, as can be seen in Figure 10(a). The phantom for DMEM was fabricated using water and salt. The quantities of ingredients used to prepare the mixtures are given in Table 1. The maximum deviation of the permittivity and the conductivity of the DMEM phantom is 4.13% and 7.91%, respectively, within the band of interest, as can be seen in Figure 10(b). A comparison of the electrical properties of the numerical and the physical phantoms for both the human muscle and DMEM phantoms are shown in Figure 10.

Finally, four versions of the biohybrid implant are prototyped. These prototypes mimic the deflection of the pillars of which mechanical simulations were presented in the section "Mechanical Model," as seen in Figure 11(b).

RESULTS AND DISCUSSION

Simulations were run with the electromagnetic model that was detailed in the section "Electromagnetic Model." The transmission coefficient between the ports of the on-body antenna changes as the implant antenna is reconfigured by the mechanical switch. As can be seen in Figure 8, the degree of deflection for 50, 100, and 300 μN as well as the switching can be tracked.

The transmission coefficient between the ports of the on-body antenna is measured while these versions are located inside the DMEM phantom. Figure 11(a) shows the change in transmission coefficient as the force generated by the muscle increases. As the force generated by the muscle increases, the capacitance between the conductive bridge and the implant antenna decreases as the bridge moves away from the antenna. It is observed that the resonance frequency in $|S_{21}|$ increases as the capacitance decreases. The measurement results are parallel to the predicted results presented in Figure 8(a). However, the dips observed in the measurements occur at a lower frequency range in the simulations. This could be due to the differences in the phantoms as well as to the imperfect prototyping of the biohybrid implants. Since the physical phantom mimics the numerical phantom in a narrow band, the change in the resonance frequency obtained in the measurement results is observed at a higher frequency than in the simulation. To tackle this unpredictable behavior, which is expected in real-life scenarios where we locate the implanted antenna in various locations inside the human body, we propose a wideband reading technique. We also did multiple trials with slight variations in the implant and the phantom. In each case, we managed to demonstrate successful detection of the implant antenna reconfiguration although variations in resonant frequency were observed. Note that the alignment between the reader antenna and
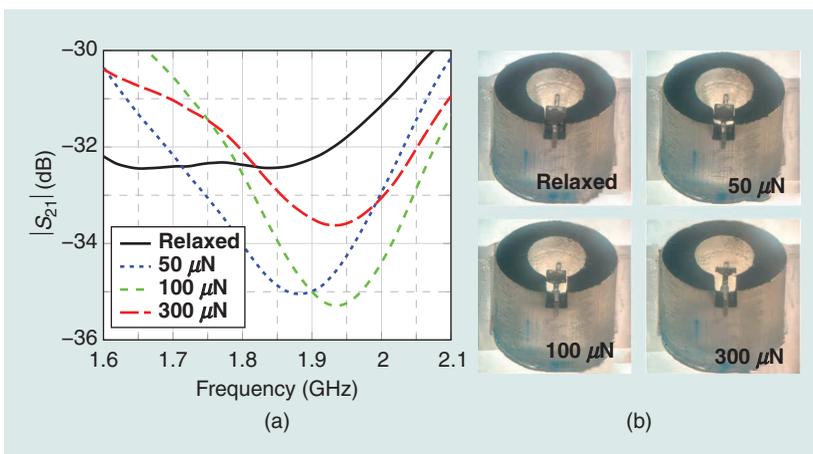
FIGURE 11. Electromagnetic measurement results for implant antennas mimicking reconfiguration under gradual muscle contraction. (a) Change in $|S_{21}|$ against the gradual contraction of the tissue. (b) implant antenna prototypes.

the implant is also critical. The sensing drastically deteriorates with misalignment, as previously reported in [43]. In the future, time-domain techniques will be utilized to mitigate this problem. The stabilization against the parasitic effects inside the body is also an open problem that should be addressed.

CONCLUSIONS

In this article, a biohybrid implant that is capable of performing sensing at a molecular level and forming a wireless link is described. The sensing is performed by engineered muscle tissue, which contracts upon reception of the trigger molecule, namely the molecule to be sensed. This contraction results in the reconfiguration of the implant antenna. Note that the implant antenna is a passive antenna that acts as a reflector. The reconfiguration causes a change in the transmission coefficient between the ports of a dual port on-body antenna. It has been shown that the reconfiguration can take place if the skeletal muscle generates 50 μN through mechanical simulation. It has also been shown that this reconfiguration can be tracked at a 1-cm depth with both simulations and phantom measurements. In the future, the overall system will be combined where the wireless tracking will take place while the 3D-engineered skeletal muscle contraction takes place with the introduction of the trigger molecule into DMEM.

SUPPLEMENTARY MATERIAL

This article has supplementary downloadable material available at https://doi.org/10.1109/MAP.2023.3320589, provided by the authors.

AUTHOR INFORMATION

Cagla Karabulut (cagla.karabulut@boun.edu.tr) is currently a master's student in electronics at Bogazici University, Istanbul 34342, Turkey, and a graduate researcher in the Bogazici University Antennas and Propagation Research Laboratory. She received her bachelor's degree in electrical and electronics engineering from Istanbul Bilgi University, Istanbul, Turkey, in 2020. She is a Student Member of IEEE.

Ahmet Bilir (ahmet.bilir@boun.edu.tr) is studying electrical and electronics engineering and mathematics at Bogazici University, Istanbul 34342, Turkey. He is an undergraduate researcher in the Bogazici University Antennas and Propagation Research Laboratory. He is a Student Member of IEEE.

Macit Emre Lacin (melacin@gmail.com) is pursuing his second postdoctoral study at the Cleveland Clinic Lerner Research Institute, Cleveland, OH 44106 USA. He received his Ph.D. degree in neuroscience from Mount Sinai School of Medicine, NY, USA. He was a postdoctoral researcher at Bogazici University from 2021 to 2022.

Sema Dumanli (sema.dumanli@boun.edu.tr) is an associate professor at Bogazici University, Istanbul 34342, Turkey, where she founded and directs the BOUNtenna Antennas and Propagation Research Laboratory and AntennAlive Biohybrid Systems Laboratory. Her research interests include antenna design for implant wearable devices. She received the IEEE APS Donald G. Dudley Jr. Award in 2022. She is a Member of IEEE.

REFERENCES

[1] S. Yim and M. Sitti, "Design and rolling locomotion of a magnetically actuated soft capsule endoscope," *IEEE Trans. Robot.*, vol. 28, no. 1, pp. 183–194, Feb. 2012, doi: 10.1109/TRO.2011.2163861.

[2] A. Karargyris and N. Bourbakis, "Detection of small bowel polyps and ulcers in wireless capsule endoscopy videos," *IEEE Trans. Biomed. Eng.*, vol. 58, no. 10, pp. 2777–2786, Oct. 2011, doi: 10.1109/TBME.2011.2155064.

[3] M. Yin, D. A. Borton, J. Aceros, W. R. Patterson, and A. V. Nurmikko, "A 100-channel hermetically sealed implantable device for chronic wireless neurosensing applications," *IEEE Trans. Biomed. Circuits Syst.*, vol. 7, no. 2, pp. 115–128, Apr. 2013, doi: 10.1109/TBCAS.2013.2255874.

[4] S. Kim et al., "Subcutaneously implantable electromagnetic biosensor system for continuous glucose monitoring," *Scientific Rep.*, vol. 12, no. 1, 2022, Art. no. 17395, doi: 10.1038/s41598-022-22128-w.

[5] J. Y. Lucisano, T. L. Routh, J. T. Lin, and D. A. Gough, "Glucose monitoring in individuals with diabetes using a long-term implanted sensor/telemetry system and model," *IEEE Trans. Biomed. Eng.*, vol. 64, no. 9, pp. 1982–1993, Sep. 2017, doi: 10.1109/TBME.2016.2619333.

[6] J. L. Gonzalez-Guillaumin, D. C. Sadowski, K. V. I. S. Kaler, and M. P. Mintchev, "Ingestible capsule for impedance and pH monitoring in the esophagus," *IEEE Trans. Biomed. Eng.*, vol. 54, no. 12, pp. 2231–2236, Dec. 2007, doi: 10.1109/TBME.2007.908332.

[7] P. A. Hammond, D. Ali, and D. R. S. Cumming, "A system-on-chip digital pH meter for use in a wireless diagnostic capsule," *IEEE Trans. Biomed. Eng.*, vol. 52, no. 4, pp. 687–694, Apr. 2005, doi: 10.1109/TBME.2005.844041.

[8] H. Y. Lee, B. Choi, S. Kim, S. J. Kim, W. J. Bae, and S. W. Kim, "Sensitivity-enhanced LC pressure sensor for wireless bladder pressure monitoring," *IEEE Sensors J.*, vol. 16, no. 12, pp. 4715–4724, Jun. 2016, doi: 10.1109/JSEN.2016.2533262.

[9] J. Malik, S. Kim, J. M. Seo, Y. M. Cho, and F. Bien, "Minimally invasive implant type electromagnetic biosensor for continuous glucose monitoring system: In vivo evaluation," *IEEE Trans. Biomed. Eng.*, vol. 70, no. 3, pp. 1000–1011, Mar. 2023, doi: 10.1109/TBME.2022.3207240.

[10] J. Hanna et al., "Noninvasive, wearable, and tunable electromagnetic multisensing system for continuous glucose monitoring, mimicking vasculature anatomy," *Sci. Adv.*, vol. 6, no. 24, 2020, Art. no. eaba5320, doi: 10.1126/sciadv.aba5320.

[11] L. W. Y. Liu et al., "In-vivo and ex-vivo measurements of blood glucose using whispering gallery modes," *Sensors (Basel)*, vol. 20, no. 3, Feb. 2020, Art. no. 830, doi: 10.3390/s20030830.

[12] S. Saha et al., "A glucose sensing system based on transmission measurements at millimetre waves using micro strip patch antennas," *Scientific Rep.*, vol. 7, no. 1, 2017, Art. no. 6855, doi: 10.1038/s41598-017-06926-1.

[13] Y. Akiyama, A. Nakayama, S. Nakano, R. Amiya, and J. Hirose, "An electrical stimulation culture system for daily maintenance-free muscle tissue production," *Cyborg Bionic Syst.*, vol. 2021, pp. 1–12, Apr. 2021, doi: 10.34133/2021/9820505.

[14] D. R. Thévenot, K. Toth, R. A. Durst, and G. S. Wilson, "Electrochemical biosensors: Recommended definitions and classification," *Biosensors Bioelectronics*, vol. 16, nos. 1–2, pp. 121–131, Jan. 2001, doi: 10.1016/S0956-5663(01)00115-4.

[15] K. J. Cash, F. Ricci, and K. W. Plaxco, "An electrochemical sensor for the detection of protein-small molecule interactions directly in serum and other complex matrices," *J. Amer. Chem. Soc.*, vol. 131, no. 20, pp. 6955–6957, May 2009, doi: 10.1021/ja9011595.

[16] N. Maccaferri et al., "Ultrasensitive and label-free molecular-level detection enabled by light phase control in magnetoplasmonic nanoantennas," *Nature Commun.*, vol. 6, no. 1, 2015, Art. no. 6150, doi: 10.1038/ncomms7150.

[17] D. Erickson, S. Mandal, A. H. J. Yang, and B. Cordovez, "Nanobiosensors: Optofluidic, electrical and mechanical approaches to biomolecular detection at the nanoscale," *Microfluidics Nanofluidics*, vol. 4, nos. 1–2, pp. 33–52, Jan. 2008, doi: 10.1007/s10404-007-0198-8.

[18] O. F. Sezgen et al., "A multiscale communications system based on engineered bacteria," *IEEE Commun. Mag.*, vol. 59, no. 5, pp. 62–67, May 2021, doi: 10.1109/MCOM.001.2000964.

[19] M. Mimee et al., "An ingestible bacterial-electronic system to monitor gastrointestinal health," *Science*, vol. 360, no. 6391, pp. 915–918, May 2018, doi: 10.1126/science.aas9315.

[20] M. Hicks, T. T. Bachmann, and B. Wang, "Synthetic biology enables programmable cell-based biosensors," *ChemPhysChem*, vol. 21, no. 2, pp. 132–144, Jan. 2020, doi: 10.1002/cphc.201900739.

[21] B. Saltepe, E. Ş. Kehribar, S. S. Su Yirmibeşoğlu, and U. Ö. Şafak Şeker, "Cellular biosensors with engineered genetic circuits," *ACS Sensors*, vol. 3, no. 1, pp. 13–26, Jan. 2018, doi: 10.1021/acssensors.7b00728.

[22] E. J. Archer, A. B. Robinson, and G. M. Suel, "Engineered E. coli that detect and respond to gut inflammation through nitric oxide sensing," *ACS Synthetic Biol.*, vol. 1, no. 10, pp. 451–457, Oct. 2012, doi: 10.1021/sb3000595.

[23] M. Mimee, A. C. Tucker, C. A. Voigt, and T. K. Lu, "Programming a human commensal bacterium, Bacteroides thetaiotaomicron, to sense and respond to stimuli in the murine gut microbiota," *Cell Syst.*, vol. 1, no. 1, pp. 62–71, Jul. 2015, doi: 10.1016/j.cels.2016.03.007.

[24] N. Gupta, V. Renugopalakrishnan, D. Liepmann, R. Paulmurugan, and B. D. Malhotra, "Cell-based biosensors: Recent trends, challenges and future perspectives," *Biosensors Bioelectronics*, vol. 141, Sep. 2019, Art. no. 111435, doi: 10.1016/j.bios.2019.111435.

[25] D. Nikolayev, A. K. Skrivervik, J. S. Ho, M. Zhadobov, and R. Sauleau, "Reconfigurable dual-band capsule-conformal antenna array for in-body bioelectronics," *IEEE Trans. Antennas Propag.*, vol. 70, no. 5, pp. 3749–3761, May 2022, doi: 10.1109/TAP.2021.3138264.

[26] Z. Bao, Y.-X. Guo, and R. Mittra, "Conformal capsule antenna with reconfigurable radiation pattern for robust communications," *IEEE Trans. Antennas Propag.*, vol. 66, no. 7, pp. 3354–3365, Jul. 2018, doi: 10.1109/TAP.2018.2829828.

[27] X.-T. Yang, H. Wong, and J. Xiang, "Polarization reconfigurable planar inverted-F antenna for implantable telemetry applications," *IEEE Access*, vol. 7, pp. 141,900–141,909, 2019, doi: 10.1109/ACCESS.2019.2941388.

[28] A. Khaleghi, A. Hasanvand, and I. Balasingham, "Radio frequency backscatter communication for high data rate deep implants," *IEEE Trans. Microw. Theory Techn.*, vol. 67, no. 3, pp. 1093–1106, Mar. 2019, doi: 10.1109/TMTT.2018.2886844.

[29] A. D. Ismailov and L. E. Aleskerova, "Photo-biosensors containing luminescent bacteria," *Biochemistry Moscow*, vol. 80, no. 6, pp. 733–744, Jun. 2015, doi: 10.1134/S0006297915060085.

[30] S. D. Oktar, "A system and method which provides wireless communication between bio-nano elements and macro/micro devices," U.S. Patent WO2021126135A1, Jun. 2021.

[31] L. Gao et al., "Recent progress in engineering functional biohybrid robots actuated by living cells," *Acta Biomaterialia*, vol. 121, pp. 29–40, Feb. 2021, doi: 10.1016/j.actbio.2020.12.002.

[32] B. Wang, M. Barahona, and M. Buck, "A modular cell-based biosensor using engineered genetic logic circuits to detect and integrate multiple environmental signals," *Biosensors Bioelectronics*, vol. 40, no. 1, pp. 368–376, Feb. 2013, doi: 10.1016/j.bios.2012.08.011.

[33] "IBT resin." Formlabs. Accessed: Dec. 21, 2022. [Online]. Available: https://dental-media.formlabs.com/ datasheets/2102519-TDS-ENUS-0.pdf

[34] K. Morishima et al., "Demonstration of a bio-microactuator powered by cultured cardiomyocytes coupled to hydrogel micropillars," *Sensors Actuators B, Chem.*, vol. 119, no. 1, pp. 345–350, Nov. 2006, doi: 10.1016/j.snb.2005.11.063.

[35] R. M. Duffy and A. W. Feinberg, "Engineered skeletal muscle tissue for soft robotics: Fabrication strategies, current applications, and future challenges," *Wiley Interdisciplinary Rev., Nanomedicine Nanobiotechnology*, vol. 6, no. 2, pp. 178–195, Mar./Apr. 2014, doi: 10.1002/wnan.1254.

[36] L. Ricotti et al., "Biohybrid actuators for robotics: A review of devices actuated by living cells," *Sci. Robot.*, vol. 2, no. 12, Nov. 2017, Art. no. eaaq0495, doi: 10.1126/scirobotics.aaq0495.

[37] A. W. Feinberg, A. Feigel, S. S. Shevkoplyas, S. Sheehy, G. M. Whitesides, and K. K. Parker, "Muscular thin films for building actuators and powering devices," *Science*, vol. 317, no. 5843, pp. 1366–1370, Sep. 2007, doi: 10.1126/science.1146885.

[38] J. Schindelin et al., "Fiji: An open-source platform for biological-image analysis," *Nature Methods*, vol. 9, no. 7, pp. 676–682, Jul. 2012, doi: 10.1038/nmeth.2019.

[39] Y. Tanaka et al., "An actuated pump on-chip powered by cultured cardiomyocytes," *Lab Chip*, vol. 6, no. 3, pp. 362–368, 2006, doi: 10.1039/B515149J.

[40] S. Ahadian et al., "Organ-on-a-chip platforms: A convergence of advanced materials, cells, and microscale technologies," *Adv. Healthcare Mater.*, vol. 7, no. 2, Jan. 2018, Art. no. 1700506, doi: 10.1002/adhm.201700506.

[41] G. Caluori et al., "Non-invasive electromechanical cell-based biosensors for improved investigation of 3D cardiac models," *Biosensors Bioelectronics*, vol. 124–125, pp. 129–135, Jan. 2019, doi: 10.1016/j.bios.2018.10.021.

[42] A. Bilir and S. Dumanli, "Wide-band dual port cross slot wearable antenna for in-body communications," in *Proc. 17th Eur. Conf. Antennas Propag. (EuCAP)*, 2023, pp. 1–5, doi: 10.23919/EuCAP57121.2023.10133068.

[43] C. Karabulut, A. Bilir, M. E. Lacin, and S. Dumanli, "Implant antenna reconfigured by engineered skeletal muscle tissue," in *Proc. 17th Eur. Conf. Antennas Propag. (EuCAP)*, 2023, pp. 1–5, doi: 10.23919/EuCAP57121.2023.10132955.

[44] T. F. Knight, "Idempotent vector design for standard assembly of biobricks," MIT Artificial Intelligence Laboratory, Cambridge, MA, USA, 2003. [Online]. Available: http://hdl.handle.net/1721.1/21168

[45] J. E. Hall, *Guyton and Hall Textbook of Medical Physiology*, 12th ed. New York, NY, USA: Elsevier, 2011.

MEETINGS & SYMPOSIA

IEEE INTERNATIONAL CONFERENCE ON COMMUNICATIONS (ICC 2024)

9–13 June 2024, Denver, CO, USA. (Papers: 11 October 2023.) Melissa Torres, senior conference planner, IEEE Communications Society, +1 212 705 8979, e-mail: m.a.torres@comsoc.org. http://icc2024.ieee-icc.org.

2024 IEEE/MTT-S INTERNATIONAL MICROWAVE SYMPOSIUM (IMS 2024)

16–21 June 2024, Washington, DC, USA. (Papers: 5 December 2023). Contact: General Information: e-mail: support@mtt.org. http://www.ims-ieee.org.

2024 IEEE INTERNATIONAL SYMPOSIUM ON ANTENNAS AND PROPAGATION & USNC-URSI RADIO SCIENCE MEETING

14–19 July 2024, Florence, Italy. (Papers: 21 January 2024). Roberto D. Graglia, conference co-chair, Politecnico di Torino, Corso Duca degli Abruzzi, 24, 10129 Torino, Italy, e-mail: roberto.graglia@polito.it. https://2024.apsursi.org.